REVIEW ARTICLE

Increased glucose metabolism by FDG-PET correlates with reduced tumor angiogenesis in oral squamous cell carcinoma

Mikiko Nakamura · Yoshimasa Kitagawa · Yutaka Yamazaki · Hironobu Hata ·
Motoko Kotsuji · Yasuhisa Fujibayashi · Hidehiko Okazawa · Yoshiharu Yonekura ·
Kazuo Sano

Abstract Hypoxia is known to have been related with angiogenesis and glycolysis, and may have an influence on tumor treatment effect. Because glucose utilization is higher in malignant cells than that in normal cells, dynamic glucose metabolism of tumor has been evaluated by means of [^{18}F]-fluorodeoxyglucose positron emission tomography (FDG-PET). To investigate the significance of tumor vascularization in oral squamous cell carcinoma, we compared tumor angiogenesis with the FDG-PET findings. Twenty patients underwent FDG-PET. For the quantitative evaluation of FDG uptake in each tumor, the mean standardized uptake value (SUV) was calculated. Microvessel structures labeled with CD34 antigen were investigated in pretreatment biopsy specimens. Using an image analyzer, we calculated the following microvessel parameters: the ratio of the total number of microvessels (TN) to tumor area (TA), the ratio of the total microvessel perimeter (TP) to the TA, and the ratio of the tumor tissue area more than 150 μm distant from each microvessel (hypoxic ratio, %).

The SUV was compared with the above parameters. Simple regression analysis revealed a statistical significance between the SUV and the TN:TA ratio ($p = 0.046$), as well as between the SUV and the TP:TA ratio ($p = 0.0206$). The SUV was found to be inversely related to the TN:TA and TP:TA ratios. Elevated glucose metabolism assessed by FDG-PET correlated with reduced vascularization. Higher glucose metabolism might therefore reflect a state of hypoxia.

Keywords Positron emission tomography (PET) · Squamous cell carcinoma · Microvessel · Angiogenesis · Hypoxia

M. Nakamura · M. Kotsuji · K. Sano
Division of Dentistry and Oral Surgery,
Department of Sensory and Locomotor Medicine,
School of Medicine, University of Fukui, Fukui, Japan

Y. Kitagawa (✉) · Y. Yamazaki · H. Hata
Oral Diagnosis and Medicine, Department of Oral
Pathobiological Science, Graduate School of Dental Medicine,
Hokkaido University, North 13, West 7, Kita-ku,
Sapporo 060-8586, Japan
e-mail: ykitagaw@den.hokudai.ac.jp

Y. Fujibayashi · H. Okazawa
Biomedical Imaging Research Center, University of Fukui,
Fukui, Japan

Y. Fujibayashi · Y. Yonekura
National Institute of Radiological Sciences, Chiba, Japan

Introduction

It is well known that glucose metabolism is accelerated in various malignant tumors, and [^{18}F]-fluorodeoxyglucose (FDG), which is an analog of glucose, is also transported easily into tumor cells via glucose transporters expressed on the cell membrane. In malignant tumors, including squamous cell carcinoma (SCC) of the head and neck, FDG uptake reflects the dynamic glucose metabolism of tumors. FDG positron emission tomography (FDG-PET) imaging is therefore useful as an excellent non-invasive diagnostic tool for tumor detection as well as for evaluating both the viability and degree of malignancy of tumors. We have previously demonstrated the clinical significance of FDG-PET in the assessment of responses to treatment and in the prediction of residual viable tumor cells after preoperative chemoradiotherapy in oral SCC [1, 2].

Histological grading has been conventionally used to evaluate the degree of malignancy and to predict the efficacy of treatment in cases of oral SCC. Although less

differentiated tumors are generally considered to possess a higher degree of malignancy, the clinical behavior and the sensitivity to chemotherapy or radiotherapy vary, even in cases involving tumors with the same type of differentiation. Due to such characteristics, it is difficult to use the conventional clinicopathological criteria in order to accurately predict tumor aggressiveness and proliferative activity. To clarify the potential biological malignancy of each tumor individually and to evaluate the possible usefulness of FDG-PET in predicting the aggressiveness of oral SCCs, we investigated the correlation between FDG-PET and certain cell cycle-associated markers (i.e., MIB-1 and proliferating cell nuclear antigen) [3] as well as the argyrophilic nucleolar organizer regions (AgNORs) score, which reflects the degree of protein synthesis [4]. These previous studies suggested that FDG-PET may provide non-invasive, functional images that are reflective of tumor aggressiveness.

The metabolism of malignant tumor cells depends on neovascularization to provide oxygen and glucose, which in turn enables tumor growth. As regards the tumor microenvironment, angiogenesis is considered to be a fundamental process in tumor growth and metastasis [5]. Moreover, angiogenesis has been considered to be one of the most important factors which influence the efficacy of radiotherapy and/or chemotherapy for the treatment of malignant tumors [6–9].

To investigate the significance of tumor vascularization in cases of oral SCC, we compared the regional uptake of FDG with tumor angiogenesis.

Materials and methods

Patients

The present study was conducted with 20 consecutive patients who underwent FDG-PET study before chemoradiotherapy for oral SCC (17 males and 3 females; mean age 62.3 years; range 47–78 years) (Table 1). The study was limited to patients with a primary carcinoma. Patients with previous treatment for cancer, distant metastasis or known diabetes mellitus were excluded from the study. Before treatment, biopsy was performed for the histopathological and immunohistochemical evaluation of all patients. Primary sites were the tongue ($n = 6$), mandibular gingiva (5), floor of the mouth (4), buccal mucosa (2), maxillary gingiva (1), hard palate (1), and lower lip (1). The protocol was approved by the Ethics Committee of the School of Medicine at the University of Fukui, and each patient provided his or her written informed consent. Clinical staging was based on the International Union Against Cancer [10] and American Joint Committee on Cancer [11]

TNM classification. Twelve of 20 patients had stage III or IV cancer. Each of 16 patients had a well-differentiated SCC, and the remaining four had a moderately differentiated SCC. FDG-PET study was performed before biopsy in all patients in order to eliminate the potential influence of the biopsy on the PET results.

Treatment regimen and clinical follow-up

All 20 patients underwent our concurrent chemoradiotherapy [1–3] (an organ preservation protocol), which consisted of 2 courses of intraarterial chemotherapy (THP-ADM, 5-FU, and carboplatin: CBDCA) and concomitant radiotherapy (30–40 Gy, 1.8–2.0 Gy per fraction, at 5 fractions a week), delivered to the primary site and involving the neck region. In 7 of 20 patients with tumors crossing the midline, the catheters were placed bilaterally.

Approximately 4 weeks after the chemoradiotherapy, the grading of clinical responses was carried out based on the World Health Organization criteria [12]. The clinical course of all patients was followed up for more than 5 years.

FDG-PET imaging

All of the patients fasted for more than 4 h before the PET study. 244–488 MBq of ^{18}FDG, synthesized with an automated FDG synthesis system (NKK, Tokyo, Japan) using a small cyclotron (OSCAR3, Oxford Instruments, Oxon, UK), was administered intravenously over a period of 10 s. The PET scanning was performed using a GE Advance System (GE, Milwaukee, WI, USA). Transmission scans were obtained for 10 min using a standard pin source of 68Ge/68Ga for attenuation correction of the emission images. The emission scan for a static image was performed for 20 min, starting 40 min after the injection. Plasma glucose levels were measured in all patients.

Data analysis of PET result

For the quantitative evaluation of FDG uptake into the tumor using the static images, regions of interest (ROI: round shape with a diameter of 5 mm) were placed in the area of highest FDG uptake on a transaxial plane. The FDG uptake values were corrected for the injected dose and the patients' weight, in order to calculate the mean standardized uptake values (mean SUVs) using the following formula:

$$SUV = \frac{\text{tissue radioactivity concentration (Bq/ml)}}{\text{injected dose (Bq)/body weight (g)}}.$$

Table 1

Patient No.	Age	Sex	Primary site	Differentiation	TNM classification	Stage	Clinical response	SUV	TN:TA	TP:TA	Hypoxic ratio	Prognosis (survival period)
1	68	M	Palatal mucosa	Moderate	T1 N 0 M 0	I	CR	9.76	32.87	1.63	17.16	Alive
2	71	M	Tongue	Well	T2 N 0 M 0	II	CR	10.56	36.88	2.19	6.80	Alive
3	70	M	Maxillary gingiva	Well	T2 N 0 M 0	II	CR	7.96	55.32	2.64	2.75	Alive
4	71	F	Tongue	Well	T2 N 0 M 0	II	CR	4.07	92.09	6.83	0.36	Alive
5	66	M	Tongue	Well	T2 N 0 M 0	II	CR	5.15	74.08	3.62	8.84	Alive
6	71	M	Floor of the mouth	Moderate	T2 N 0 M 0	II	CR	6.60	129.06	5.20	0.00	Died of second cancer (38 months)
7	78	M	Floor of the mouth	Well	T2 N 0 M 0	II	CR	10.46	14.29	0.94	25.11	Alive
8	51	F	Tongue	Moderate	T2 N 0 M 0	II	PR	8.54	128.45	5.03	2.17	Alive
9	47	M	Lower lip	Well	T2 N 1 M 0	III	CR	11.22	72.04	4.44	0.07	Alive
10	48	M	Mandibular gingiva	Well	T2 N 1 M 0	III	CR	7.70	60.67	2.29	2.13	Alive
11	63	M	Buccal mucosa	Well	T3 N 0 M 0	III	CR	5.59	37.34	1.84	17.66	Died of gastric cancer (28 months)
12	74	M	Floor of the mouth	Well	T3 N 1 M 0	III	CR	14.54	40.11	2.20	6.81	Died of pneumonia (13 months)
13	66	M	Buccal mucosa	Well	T3 N2b M 0	IV	CR	5.07	27.91	1.91	14.54	Alive
14	64	M	Mandibular gingiva	Well	T4 N 0 M 0	IV	CR	8.40	67.70	3.00	11.72	Alive
15	56	M	Floor of the mouth	Well	T4 N 0 M 0	IV	CR	26.10	47.91	1.47	12.81	Alive
16	58	M	Mandibular gingiva	Well	T4 N 0 M 0	IV	PR	11.34	129.65	3.28	4.28	Alive
17	50	M	Tongue	Well	T4 N 1 M 0	IV	CR	14.12	80.92	1.47	4.08	Died of lung cancer (11 months)
18	51	M	Mandible	Moderate	T4 N 1 M 0	IV	PR	7.28	48.05	5.38	0.48	Alive
19	60	M	Mandibular gingiva	Well	T4 N2a M 0	IV	PR	12.77	47.48	0.73	4.90	Alive
20	63	F	Tongue	Well	T4 N2b M 0	IV	PR	7.85	28.09	1.12	25.89	Died of unknown disease (45 months)
Mean ± SD								9.75 ± 4.85 mg/ml	62.55 ± 34.67 vessels/mm^2	8.43 ± 8.10 mm/mm^2	2.86 ± 1.71%	

Well well differentiated squamous cell carcinoma, *moderate* moderately differentiated squamous cell carcinoma, *CR* complete response, *PR* partial response, *TN:TA* total microvessel number:total tumor area, *TP:TA* total microvessel perimeter:total tumor area

Fig. 1 Image analysis. **a** Low-power view of hematoxylin–eosin staining showing invasive growth of tumor cells (×13.2). **b** Immunohistochemical staining for CD34 in SCC biopsy specimens. Note the intense staining of the endothelial cells in these vessels. **c** The outlines of the tumor and of the endothelium of each microvessel are traced on a computer display. The total number of microvessels and the total microvessel perimeters have been calculated. **d** The *yellow circle* indicates the oxygenated area within 150 μm of a microvessel. The ratio of tumor tissue in an area extending beyond 150 μm from the microvessel was calculated as hypoxic ratio in each case
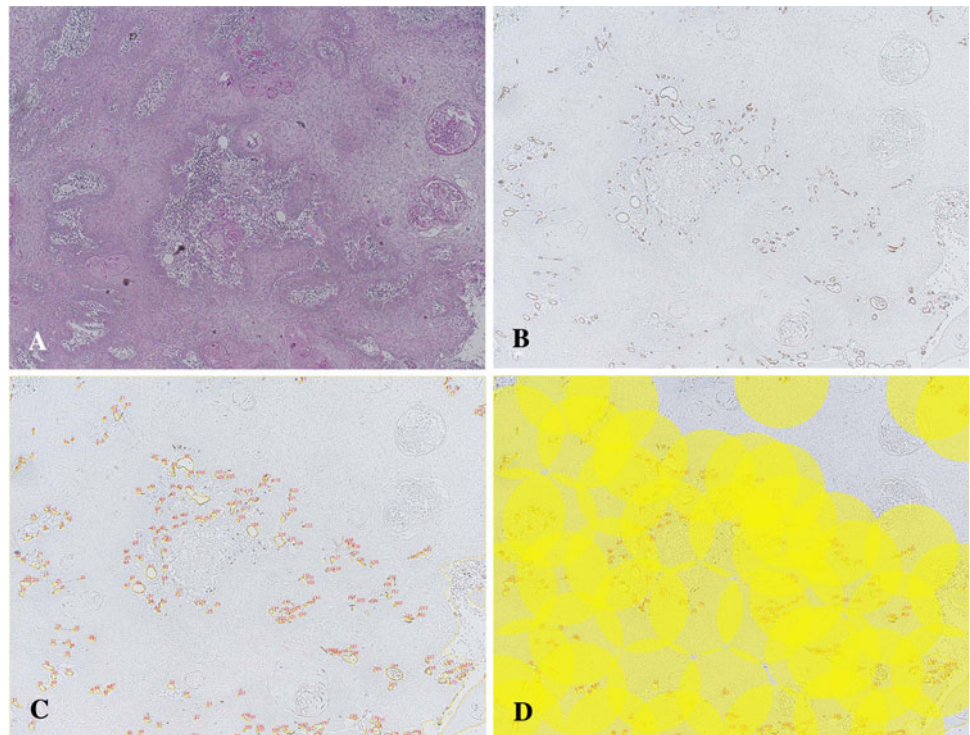
Immunohistochemical staining

It is generally accepted that CD34 monoclonal antibody, which specifically reacts with *Homo sapiens* hematopoietic stem-cell antigens, is useful for identification of vascular endothelium cells by immunohistochemical staining of formalin-fixed, paraffin-embedded sections.

Here, the tumors were fixed in 10% buffered formalin overnight. Serial tissue sections (4 μm) were deparaffinized and antigen retrieval was carried out in an autoclave for 15 min at 121°C in 0.01 M citrate buffer (pH 6.0). After washing the sections in distilled water, they were immersed in 0.3% H_2O_2 methanol in order to quench any endogenous peroxidase activity. Then, the sections were washed in PBS and were incubated for 20 min with diluted normal blocking serum.

Microvessels were evaluated using a monoclonal antibody against CD34 class II antigen (clone QBEnd 10; DAKO, Carpinteria, CA, USA). The primary antibody was diluted to 1:50 with PBS, and sections were incubated for 60 min at room temperature. Specific immunostaining was detected by the formation of avidin–biotin complexes using a VECTASTAIN Elite ABC KIT (Vector Laboratories Inc., Burlingame, CA) and diaminobenzidine (Dojindo, Kumamoto, Japan). Finally, counterstaining with Mayer's hematoxylin was performed.

Angiogenesis assessment

Microvessel structures labeled with CD34 antigen were investigated in all samples (Fig. 1a, b). The area of highest vascularization was chosen at low-power magnification (13.2×) in individual immunohistochemically stained sections. In the selected areas, we calculated the following factors using a image analyzer software (Mac-SCOPE, Mitani Corp., Fukui, Japan) and graphic soft (Adobe Photoshop 5.0) for Macintosh (BNN, Tokyo, Japan) as previously described by Kamijo et al. [8]. The outlines of the endothelium of each microvessel and of the tumor biopsy specimen are traced on a computer display (Fig. 1c). They were converted to binary images, and the total microvessel number (TN), the total perimeter of the microvessels (TP), and total tumor tissue area (TA) were calculated in each of the 20 cases. TN divided by TA is the TN:TA ratio, and TP divided by TA is the TP:TA ratio.

(a) the ratio of the total microvessel number (TN) to tumor area (TA)

$$TN:TA = \frac{tumor\ microvessel\ number\ (TN)}{tumor\ area\ (TA, mm^2)}$$

(b) The ratio of the total microvessel perimeter (TP) to TA

Fig. 2 Patient no. 11.
a Intraoral photograph of an primary well-differentiated squamous cell carcinoma of left buccal mucosa. **b** FDG PET image (axial plane) showing an increased uptake (*arrow*) in the left buccal region consistent with tumor
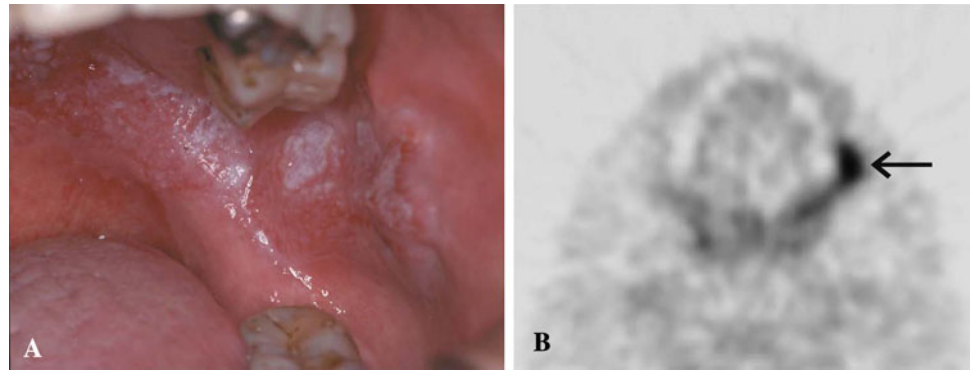
$$TP{:}TA = \frac{\text{tumor microvessel perimeter (TP)}}{\text{tumor area (TA, mm}^2)}$$

Figure 1d shows the yellow painted area within 150 μm from microvessels. The oxygen diffusion distance in tumor tissue around vessels is ~150 μm, and the ratio of tumor tissue beyond 150 μm from microvessels was calculated in each of the 20 cases (hypoxic ratio, %).

(c) Hypoxic ratio (%) = the ratio of tumor tissue area > 150 μm from microvessels.

Statistical analysis

The data presented in this paper were expressed as mean ± SD. Differences in FDG uptake were compared using a regression analysis and the Mann–Whitney U test. A regression analysis was used to determine the relationship between the SUVs and the microvessel parameters (TN:TA, TP:TA, hypoxic ratio).

All statistical analyses were performed using StatView 5.0 for Macintosh (BNN, Tokyo, Japan), and a probability value of less than 0.05 was considered to be statistically significant.

Results

Clinical response and prognosis

In all cases, the tumor decreased in size or completely disappeared macroscopically and on MR images. In terms of the WHO criteria, 15 patients showed a complete clinical response, and the remaining 5 patients showed a partial response (clinical complete response rate = 75.0%, overall response rate = 100%). Patients were followed up for 5 years. No local recurrence was observed in any of the patients and 16 patients (75%) were alive at 5-year follow-up. Two patients died of a second cancer, one died of pneumonia, and one died of unknown disease (Table 1).

SUV

In all patients, the pretreatment FDG-PET images demonstrated an increased uptake of FDG corresponding to the known primary lesion, as compared to that of the background tissues (Fig. 2).

Microvessel parameters

The microvessels in all biopsy specimens were stained with a CD34 antibody. On the computed images, TN:TA, TP:TA, and the hypoxic ratio were calculated; TN:TA = 62.55 ± 34.67 vessels/mm^2, TP:TA = 2.86 ± 1.71 mm/mm^2, hypoxic ratio = 8.43 ± 8.10% (Fig. 1).

Regression analysis results

Simple regression analysis revealed a statistical significance not only between the SUV and TN:TA, but also between the SUV and TP:TA (Eqs. 1, 2). The SUV was in inverse proportion to both the TN:TA (Fig. 3) and the TP:TA ratio (Fig. 4).

$$SUV = 13.702 - 0.063 \times (TN{:}TA) \quad (p = 0.0460) \quad (1)$$

$$SUV = 13.927 - 1.459 \times (TP{:}TA) \quad (p = 0.0206) \quad (2)$$

Tumors with higher SUVs (>9.0) had fewer microvessels per unit area of tumor ($p = 0.0016$) (Fig. 5), and they also tended to exhibit a lower TP:TA ($p = 0.0724$). The microvessel parameters and SUVs showed no correlation with clinical response to chemoradiotherapy and prognosis (Figs. 3, 4).

Discussion

It is well known that angiogenesis supplies neoplasms with O_2, and nutrition is indispensable for the proliferation, invasion, and metastasis of tumors. In fact, in cases of oral SCC with lymph node metastasis, the genes expressed at high levels included angiogenesis-related molecules [13].
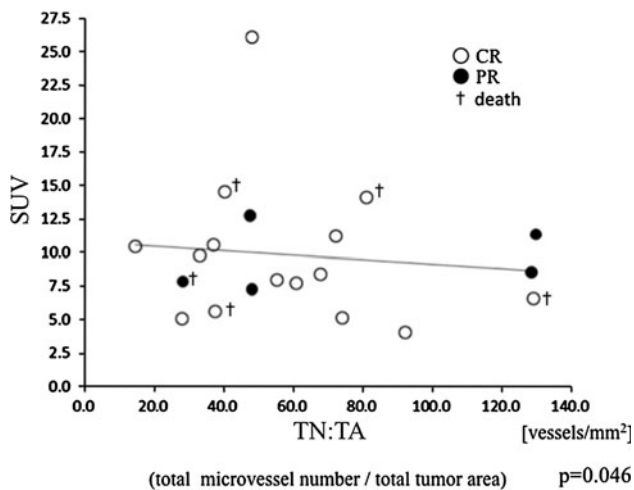
Fig. 3 Correlation of SUV with total microvessel number per total tumor area (TN:TA ratio) in 20 oral squamous cell carcinomas. SUV was in inverse proportion to the TN:TA ratio
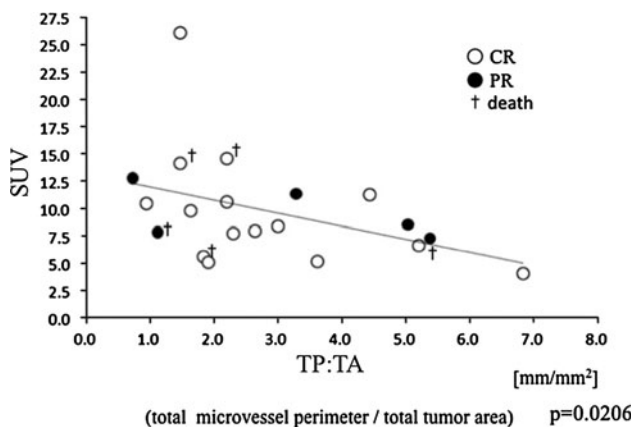

Fig. 4 Correlation of SUV with total microvessel perimeter per total tumor area (TP:TA ratio) in 20 oral squamous cell carcinomas. SUV was in inverse proportion to the TP:TA ratio
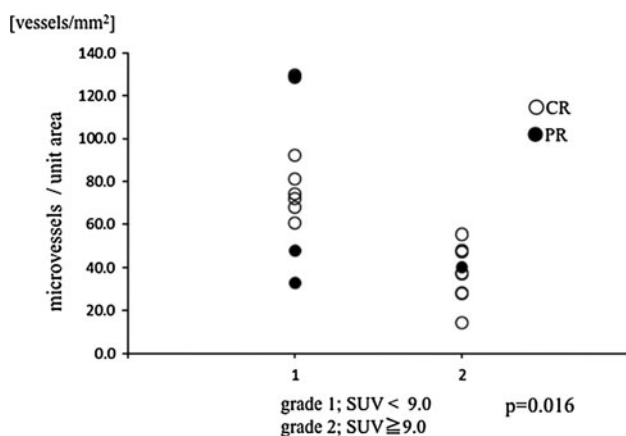

Fig. 5 Comparison of the numbers of microvessels per unit area according to the grading of SUV. Tumors with higher SUVs (>9.0) had fewer microvessels per unit area of tumor

In this context, two main factors are considered to induce tumor angiogenesis. One of these factors is the abnormal manifestation of certain oncogenes or tumor suppressor genes, and the other factor consists of changes in the tumor tissue microenvironment (hypoxia, athrepsia, acidosis, etc.). In particular, changes in the rate of glucose uptake in rapidly growing cancer cells are likely to be associated with adaptation to hypoxia, which induces a metabolic switch from oxidative to glycolytic metabolism [14]. Hypoxia has been shown to be an important stimulus for new blood vessel formation in a number of pathological conditions, including coronary artery disease, diabetic neovascularization, and tumor angiogenesis [15]. Sun et al. [16] showed that hypoxia-inducible factor-1 (HIF1)-mediated regulation of semaphorin 4D affects tumor growth and vascularity in head and neck SCC. In recent years, high levels of HIF1-alpha expression seem to predict a poor or good prognosis for various cancers, and the prognostic relevance of HIF1-alpha in tumors derived from squamous epithelium is controversial [17, 18].

Clinically, blood flow to a tumor (i.e., the degree of tissue oxygenation) is thought to be an important factor influencing the effects of both radiotherapy and certain types of chemotherapy used to treat malignant tumors. Currently, one of the most widely used methods for the assessment of tumor vascularization is the analysis of intratumoral microvessel density (MVD), i.e., the number of microvessels in a unit area. MVD is used as an index of tumor angiogenesis, and has been investigated in terms of whether or not it is related to prognosis, tumor metastasis, tumor recurrence, the ability of tumor proliferation, and treatment effects in various tumors. Many studies have indicated that the MVD value is a good predictor of prognosis (disease free survival and/or overall survival) [19–21]. And the presence and distribution pattern of CD34, indicated angiogenesis, around tumor blood vessels were also associated with early metastasis to lymph nodes, death [22], or recurrence [23].

For proliferation, tumors depend on angiogenesis; however, tumor vessels display entirely different features, compared with those of vessels in normal tissues. In particular, vessels associated with tumors are frequently extended and/or leaky, and blood flow to tumors is oftentimes irregular and can even come to a standstill; in addition, backward flow has also been reported [24, 25]. Recently, Hida et al. [26, 27] have demonstrated the new concept of "tumor endothelial cells" which can acquire cytogenetic abnormalities while in the tumor microenvironment. Therefore, functional evaluation may not be possible, even if the degree of tumor angiogenesis is evaluated only by the MVD histologically. In order to more accurately evaluate tissue oxygenation in tumors, and to overcome the limitations associated with the use of

two-dimensional biopsy specimens, Kamijo et al. [8] used a computed image system of analysis. According to their approach, the following parameters of tissue oxygenation are calculated: MVD, the ratio of the total number of microvessels (TN) to tumor area (TA), the ratio of the total microvessel perimeter (TP) to TA, and the ratio of the tumor tissue area more than 150 μm distant from each microvessel (hypoxic ratio, %). The oxygen diffusion distance in the tumor tissue surrounding vessels is considered to be 150 μm, according to Eric et al. [28]. Kamijo et al. revealed that radiosensitivity could be effectively predicted on the basis of the ratio of the total microvessel perimeter observed in the early stages of laryngeal carcinoma [8].

The issue of the relationship between FDG uptake within tumors and hypoxia had already been addressed by several authors [29, 30]. However, to date, no study has successfully clarified the correlation between vascularity and glucose metabolism in primary oral SCC. In order to elucidate the association between these factors, and to examine whether or not angiogenesis would exert an effect on the present treatment protocol, we analyzed the relationship between the SUVs and microvessel parameters in a study similar to that of Kamijo et al. [8]. Consequently, a noteworthy result was obtained.

Among the oral SCCs studied here, tumors with a higher SUV had lower TN:TA and TP:TA ratios. Tateishi et al. [31] revealed that the mean SUV of lung cancers, including 18 adenocarcinomas and 12 SCCs, correlated with the mean MVD. However, Veronesi et al. [32] revealed that no correlation was observed between neoangiogenesis and glucose metabolism in cases of lung metastases. Our results provide further support for the conclusion that glucose metabolism is activated by hypoxia, and FDG is easily taken into the neoplasm by passive diffusion, rather than by direct supply from blood vessels. As pointed out by Arsham et al. [33], from the standpoint of cellular survival, hypoxia would require the presence of a metabolic switch from oxidative to glycolytic metabolism, and to ensure further O_2 delivery, angiogenesis would be activated primarily by the vascular endothelial growth factors induced by hypoxia. In other words, our results suggest that increased glucose metabolism precedes angiogenesis as a functional change in tumors possessing the ability to grow rapidly.

FDG-PET provides the ability to assess multiple physiological aspects of tumors in the living body. The present findings suggest that elevated glucose metabolism, as assessed by FDG-PET, was correlated with reduced vascularization. In other words, increased glucose metabolism may reflect hypoxia. Several studies have linked FDG uptake in tumor to aggressiveness, resistance to treatment and poor prognosis in a wide variety tumor subsites.

However, the PET tracer FDG is not a surrogate tracer for tumor hypoxia, directly [34], and various molecular imaging of hypoxia exist and are expected to provide the selection of head and neck cancer treatment based on an individual's tumor oxygenation status [35, 36]. Further clarification of the correlations among glycolysis, angiogenesis, and clinical factors may increase the usefulness of molecular imaging involving FDG-PET and may help in the development of efficient anticancer therapies.

References

1. Kitagawa Y, Sadato N, Azuma H, Ogasawara T, Yoshida M, Ishii Y, Yonekura Y. FDG PET to evaluate combined intra-arterial chemotherapy and radiotherapy of head and neck neoplasms. J Nucl Med. 1999;40:1132–7.
2. Kitagawa Y, Nishizawa S, Sano K, Ogasawara T, Nakamura M, Sadato N, Yoshida M, Yonekura Y. Prospective comparison of 18F-FDG PET with conventional imaging modalities (MRI, CT, and 67Ga scintigraphy) in assessment of combined intraarterial chemotherapy and radiotherapy for head and neck carcinoma. J Nucl Med. 2003;44:198–206.
3. Kitagawa Y, Sano K, Nishizawa S, Nakamura M, Ogasawara T, Sadato N, Yonekura Y. FDG-PET for prediction of tumour aggressiveness and response to intra-arterial chemotherapy and radiotherapy in head and neck cancer. Eur J Nucl Med Mol Imaging. 2003;30:63–71.
4. Nakamura M, Sano K, Kitagawa Y, Ogasawara T, Nishizawa S, Yonekura Y. Diagnostic significance of FDG-PET and argyrophilic nucleolar organizer regions (AgNORs) in oral squamous cell carcinoma. Oral Oncol. 2004;40(2):190–8.
5. Tae K, El-Naggar AK, Yoo E, Feng L, Lee JJ, Hong WK, Hittelman WN, Shin DM. Expression of vascular endothelial growth factor and microvessel density in head and neck tumorigenesis. Clin Cancer Res. 2000;6(7):2821–8.
6. Harrison L, Blackwell K. Hypoxia and anemia: factors in decreased sensitivity to radiation therapy and chemotherapy? Oncologist. 2004;9:31–40.
7. Ito Y, Kamijo T, Yokose T, Kawashima M, Ogino T, Ikeda H, Hayashi R, Sasaki S, Ochiai A. Microvessel density predicts the radiosensitivity of metastatic head and neck squamous cell carcinoma in cervical lymph nodes. Int J Oncol. 2001;19:1127–32.
8. Kamijo T, Yokose T, Hasebe T, Yonou H, Hayashi R, Ebihara S, Ochiai A. Image analysis of microvessel surface area predicts radiosensitivity in early-stage laryngeal carcinoma treated with radiotherapy. Clin Cancer Res. 2001;7:2809–14.
9. Marioni G, Marino F, Giacomelli L, Staffieri C, Mariuzzi ML, Violino E, De Filippis C. Endoglin expression is associated with poor oncologic outcome in oral and oropharyngeal carcinoma. Acta Otolaryngol. 2006;126:633–9.
10. Hermanek P, Sobin LH. UICC: TNM classification of malignant tumours. 4th ed. Berlin: Springer; 1987.
11. Freming ID, Cooper JS, Henson DE. AJCC cancer staging manual. 5th ed. Philadelphia: Lippincott Williams & Wilkins; 1997.
12. WHO Handbook for reporting result of cancer treatment. WHO offset publication 48. Geneva: World Health Organization; 1979.

13. Kashiwazaki H, Hassan NM, Hamada J, Moriuchi T, Yamazaki Y, Tei K, Totsuka Y, Inoue N. Gene expression profile changes correlated with lymph node metastasis in oral squamous cell carcinoma. Odontology. 2008;96:38–43.

14. Kuiper RA, Schellens JH, Blijham GH, Beijnen JH, Voest EE. Clinical research on antiangiogenic therapy. Pharmacol Res. 1998;37:1–16.

15. Levy AP, Levy NS, Goldberg MA. Post-transcriptional regulation of vascular endothelial growth factor by hypoxia. J Biol Chem. 1996;271:2746–53.

16. Sun Q, Zhou H, Binmadi NO, Basile JR. Hypoxia-inducible factor-1-mediated regulation of semaphorin 4D affects tumor growth and vascularity. J Biol Chem. 2009;284:32066–74.

17. Koukourakis MI, Giatromanolaki A, Sivridis E, Simopoulos C, Turley H, Talks K, Gatter KC, Harris AL. Hypoxia-inducible factor (HIF1A and HIF2A), angiogenesis, and chemoradiotherapy outcome of squamous cell head-and-neck cancer. Int J Radiat Oncol Biol Phys. 2002;53:1192–202.

18. Fillies T, Werkmeister R, van Diest PJ, Brandt B, Joos U, Buerger H. HIF1-alpha overexpression indicates a good prognosis in early stage squamous cell carcinomas of the oral floor. BMC Cancer. 2005;5:84.

19. Niedergethmann M, Hildenbrand R, Wostbrock B, Hartel M, Sturm JW, Richter A, Post S. High expression of vascular endothelial growth factor predicts early recurrence and poor prognosis after curative resection for ductal adenocarcinoma of the pancreas. Pancreas. 2002;25:122–9.

20. Pignataro L, Carboni N, Midolo V, Bertolini F, Buffa R, Cesana BM, Neri A, Viale G, Pruneri G. Clinical relevance of microvessel density in laryngeal squamous cell carcinomas. Int J Cancer. 2001;92:666–70.

21. Uzzan B, Nicolas P, Cucherat M, Perret GY. Microvessel density as a prognostic factor in women with breast cancer: a systematic review of the literature and meta-analysis. Cancer Res. 2004;64:2941–55.

22. Nagatsuka H, Hibi K, Gunduz M, Tsujigiwa H, Tamamura R, Sugahara T, Sasaki A, Nagai N. Various immunostaining patterns of CD31, CD34 and endoglin and their relationship with lymph node metastasis in oral squamous cell carcinomas. J Oral Pathol Med. 2005;34:70–6.

23. Kademani D, Lewis JT, Lamb DH, Rallis DJ, Harrington JR. Angiogenesis and CD34 expression as a predictor of recurrence in oral squamous cell carcinoma. J Oral Maxillofac Surg. 2009;67:1800–5.

24. Helmlinger G, Yuan F, Dellian M, Jain RK. Interstitial pH and pO_2 gradients in solid tumors in vivo: high-resolution measurements reveal a lack of correlation. Nat Med. 1997;3:177–82.

25. Less JR, Skalak TC, Sevick EM, Jain RK. Microvascular architecture in a mammary carcinoma: branching patterns and vessel dimensions. Cancer Res. 1991;51:265–73.

26. Hida K, Hida Y, Amin DN, Flint AF, Panigrahy D, Morton CC, Klagsbrun M. Tumor-associated endothelial cells with cytogenetic abnormalities. Cancer Res. 2004;64:8249–55.

27. Hida K, Klagsbrun M. A new perspective on tumor endothelial cells: unexpected chromosome and centrosome abnormalities. Cancer Res. 2005;65:2507–10.

28. Eric JH. Predictive assays. In: Eric JH, editor. Radiology for the radiologist. 4th ed. Philadelphia: J.B. Lippincott Company; 1994. p. 130–50.

29. Busk M, Horsman MR, Kristjansen PE, van der Kogel AJ, Bussink J, Overgaard J. Aerobic glycolysis in cancers: implications for the usability of oxygen-responsive genes and fluorodeoxy-glucose-PET as markers of tissue hypoxia. Int J Cancer. 2008;122:2726–34.

30. Kelly C, Smallbone K, Brady M. Tumour glycolysis: the many faces of HIF. J Theor Biol. 2008;254:508–13.

31. Tateishi U, Nishihara H, Tsukamoto E, Morikawa T, Tamaki N, Miyasaka K. Lung tumors evaluated with FDG-PET and dynamic CT: the relationship between vascular density and glucose metabolism. J Comput Assist Tomogr. 2002;26:185–90.

32. Veronesi G, Landoni C, Pelosi G, Picchio M, Sonzogni A, Leon ME, Solli PG, Leo F, Spaggiari L, Bellomi M, Fazio F, Pastorino U. Fluoro-deoxi-glucose uptake and angiogenesis are independent biological features in lung metastases. Br J Cancer. 2002;86:1391–5.

33. Arsham AM, Plas DR, Thompson CB, Simon MC. Phosphatidylinositol 3-kinase/Akt signaling is neither required for hypoxic stabilization of HIF-1 alpha nor sufficient for HIF-1-dependent target gene transcription. J Biol Chem. 2002;277:15162–70.

34. Christian N, Deheneffe S, Bol A, De Bast M, Labar D, Lee JA, Grégoire V. Is (18)F-FDG a surrogate tracer to measure tumor hypoxia? Comparison with the hypoxic tracer (14)C-EF3 in animal tumor models. Radiother Oncol. 2010;97:183–8.

35. Isa AY, Ward TH, West CM, Slevin NJ, Homer JJ. Hypoxia in head and neck cancer. Br J Radiol. 2006;79:791–8.

36. Krohn KA, Link JM, Mason RP. Molecular imaging of hypoxia. J Nucl Med. 2008;49:129S–48S.